Journal of Drug Delivery Science and Technology 60 (2020) 101995

Contents lists available at ScienceDirect

Journal of Drug Delivery Science and Technology

journal homepage: www.elsevier.com/locate/jddst

Research paper

Pulmonary administration of resveratrol/hydroxypropyl-β-cyclodextrin inclusion complex: *in vivo* disposition and *in vitro* metabolic study

Dexuan Kong [a], Chang Ren [a], Chen Ning [a], Yujie Cheng [a], Hui Cai [a], Han Xing [b], Yongjie Zhang [a], Ning Li [c], Yang Lu [a], Xijing Chen [a,*], Di Zhao [a,**]

[a] Clinical Pharmacokinetics Laboratory, China Pharmaceutical University, Nanjing, Jiangsu, 211198, China
[b] Department of Pharmacy, The First Affiliated Hospital of Zhengzhou University, Zhengzhou, 450052, China
[c] National Experimental Teaching Demonstration Center of Pharmacy, China Pharmaceutical University, Nanjing, Jiangsu, 211198, China

ARTICLE INFO

Keywords:
Pulmonary administration
Resveratrol
Pharmacokinetics
Tissue distribution
Lung disposition
Metabolism

ABSTRACT

Until today, the clinical application of phytochemicals is still limited largely due to poor oral bioavailability. Pulmonary administration is considered as an attractive alternative to oral delivery as it can improve the pharmacokinetic properties of compounds with extensive metabolism. In this study, resveratrol was selected as a study model to evaluate the feasibility of pulmonary administration in the delivery of phytochemicals, aiming to promote their therapeutic potential. The pharmacokinetic investigation on resveratrol was conducted in rats. Compared with oral delivery, resveratrol in rats after pulmonary administration showed superior absorption and bioavailability (92.95%). Directed delivery of resveratrol to lungs also showed potential usefulness in the treatment of lung diseases as drugs rapidly accumulated in lung tissues and concentrations were more than 100 times those of oral delivery at early time points. The metabolic study was carried out using rat microsomes and showed that metabolic activity of lung was much lower than that of liver. The overall results indicate that pulmonary administration is an effective strategy for both systemic and local delivery of resveratrol.

1. Introduction

Phytochemicals derived from plants is of great value for development as nutritional and pharmaceutical agents. Resveratrol (RES, Fig. 1) is one of the most extensively studied phytochemicals, being abundant in plant foods such as grapes, and peanuts [1]. The human health benefits of it have been widely investigated since the reveal of "the French Paradox" in the early 1990s [2]. To date, various *in vitro* and *in vivo* studies have reported a broad range of desirable activities of RES such as antioxidant, anti-inflammatory, cardioprotective, and anti-cancer [2,3].

Lung disease remains a worldwide public health issue with high morbidity and mortality. RES has shown the potential against some lung diseases including chronic obstructive pulmonary diseases (COPD) and lung cancer. Recent studies reported that RES can scavenge oxygen-derived free radicals and inhibit the releases of inflammatory cytokines from alveolar macrophages in COPD [4]. In the treatment of lung cancer, RES has shown the ability to inhibit cancerous cell initiation, promotion, and progression [5]. Besides, RES can also be used to treat pulmonary arterial hypertension because of its capacity to inhibit the production and secretion of MCP-1 in vascular endothelial cells [6]. In spite of these positive activities, the clinical translation of RES is largely hampered since only a small proportion of drugs could reach the lungs after conventional administration. Another problem with RES is limited bioavailability. Previous studies demonstrated that the oral bioavailability of RES in human is almost zero mainly due to the first-pass metabolism [7]. As a polyphenolic compound, RES is susceptible to phase II metabolism catalyzed by UDP-glucuronosyltransferase (UGT) and resveratrol-3-*O*-glucuronide (R3G) was reported as the most abundant metabolite in human and animals [8,9]. Because glucuronidation can reduce permeability of cell to drugs and contribute to their excretion [5], the elimination of RES from the body is extremely fast, and thus it is hard to maintain the therapeutically relevant level at action sites.

To tackle these limitations, we evaluated the pulmonary route of RES. Pulmonary administration is a non-invasive method considered as

* Corresponding author. Clinical Pharmacokinetics Laboratory, School of Basic Medicine and Clinical Pharmacy, China pharmaceutical University, #639 Longmian Avenue, Jian gnin g District, Nanjing, 211198, China.
** Corresponding author. Clinical Pharmacokinetics Laboratory, School of Basic Medicine and Clinical Pharmacy, China pharmaceutical University, #639 Longmian Avenue, Jian gnin g District, Nanjing, 211198, China.
E-mail addresses: chenxj-lab@hotmail.com (X. Chen), zh_d99@cpu.edu.cn (D. Zhao).

https://doi.org/10.1016/j.jddst.2020.101995
Received 14 May 2020; Received in revised form 20 July 2020; Accepted 31 July 2020
Available online 15 August 2020

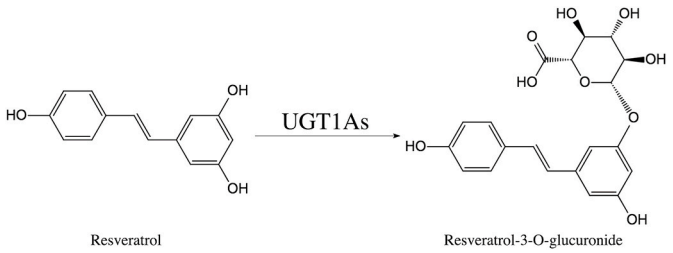

Fig. 1. Chemical structure of resveratrol (*trans*-3,5,4′-trihydroxystilbene, RES) and resveratrol-3-*O*-glucuronide (R3G). The glucuronidation was catalyzed by UDP-glucuronosyltransferase (UGT).

an alternative to oral and parenteral routs. As a local access, it is an effective approach for targeted delivery to lungs and is desirable for treating lung-specific disease states [10]. It can also provide a direct and quick access of drug into systemic circulation because of the tremendous surface area and extensive vascularization in lungs. Additionally, as the enzyme activity is relatively low in lungs, pulmonary route is a promising delivery route for compounds with extensive metabolism to circumvent hepatic and intestinal first-pass effect [11]. Benefited from these advantages, researchers have developed some inhalable formulations for delivery of RES. Valentina et al. prepared a respirable RES dry powder formulation, showing good antioxidant and anti-inflammatory activates *in vitro* [4]. A recent work from Gyeungyun et al. reported the preparation of an inhalable micelle loading RES and higher anti-inflammatory effect of that in the acute lung injury animal model [12]. Although pharmacological activities of inhalable RES have been investigated *in vitro* and *in vivo*, there is little work directed toward the pharmacokinetic characters of RES after pulmonary administration, which is also an important factor for the development of drug.

In this study, we investigated the pharmacokinetic behavior of RES after pulmonary administration to evaluate the potential of this route in the delivery of RES. The pharmacokinetic profile was evaluated in rats. RES/hydroxypropyl-β-cyclodextrin (HP-β-CD) inclusion complex was prepared and used as dosing formulation to resolve the problem of dissolution, since HP-β-CD can enhance the hydrophilicity of poorly soluble compounds through the formation of inclusion complex [13]. To further explore the metabolism mechanism of RES after pulmonary administration, metabolic profiles of it were investigated *in vitro* using rat liver microsomes and lung microsomes. Hopefully, the information obtained in this study will contribute to the further development and clinical application.

2. Materials and methods

2.1. Chemicals and regents

Resveratrol ($C_{14}H_{12}O_3$, purity>95%) and resveratrol-3-*O*-glucuronide ($C_{20}H_{20}O_9$, purity>95%) were purchased from Keweichem (Shanghai, China) and Glpbio (Montclair, America), respectively. Chlorzoxazone ($C_7H_4ClNO_2$, purity≥99%) was obtained from Sigma (Munich, Germany). Hydroxypropyl-β-cyclodextrin (HP-β-CD) was provided by J&K® (China). Lactic acid was of analytical grade and purchased from Nanjing Chemical Reagent Co., Ltd (Nanjing, China). Uridine 5′-diphosphoglucuronic acid (UDPGA, trisodium salt) was purchased from Sigma (Munich, Germany). Methanol and acetonitrile of HPLC grade were purchased from Tedia company (Fairfield, USA). Purified water used for UPLC-MS/MS analysis was produced by a Milli-Q water purification system (Millipore, Bedford, USA).

2.2. Animals

Sprague-Dawley rats were purchased from the animal center of Qinglong mountain (Nanjing, China). Rats were housed under standard conditions with a 12 h on/12 h off light cycle. During the acclimatization period, animals were raised with free access to water and chow. All experimental procedures and protocols were approved by the Animal Ethics Committee of China Pharmaceutical University (Nanjing, China).

2.3. Pharmacokinetics study

To access pharmacokinetic characters of RES after pulmonary or gastric administration, four different dosing routes were employed including intravenous (i.v), intragastric (i.g), intratracheal (i.t), and inhalable (i.h) administration. The dosing formulation of RES was prepared with 0.3 M HP-β-CD and 1% lactic acid. In brief, the excess amounts of RES were added to the aqueous solution containing 0.3 M HP-β-CD and 1% lactic acid. The mixture was continuously shaken at room temperature for 24 h to reach complete solubilization. After filtering to remove the undissolved RES, the resulting solution was freeze-dried. The obtained lyophilized complex powders were dissolved in distilled water to obtain dosing solution at 20 mg/mL of RES before animal experiments.

Animals were fasted for 12 h before the experiment and were randomly allocated to four groups (n = 5). Rats in Group I and II received RES via bolus tail vein injection (10 mg/kg) and gavage (50 mg/kg), respectively. The pulmonary administration was carried out through two different ways in the other two groups. For Group III, i. t instillation was conducted through orotracheal intubation at 20 mg/kg. Rat was anesthetized first and kept at approximately 60° angle of tilt on restraining board. After that, the tongue of animal was pulled out using forceps, and then solution was instilled into the trachea using a syringe equipped with a gavage needle followed by insufflation of an air bolus. While in Group IV, a small animal nose-only inhalation exposure system (HRH-MNE3026, Huironghe Technology) was used to achieve i. h administration of RES. That is a computer-assisted inhalation device, in which aerosol is produced through interplay between a vacuum and pressurized air gas by a controlled valve system. Each rat was placed in a restraining tube and held in place by a plunger. During the inhalation, tubes containing unanesthetized animals were connected to exposure ports of the device. Rats inhaled the aerosols at an air flow rate of 12 L/min for 100 min continuously. The concentration of RES aerosols in exposure system was measured using a filter connected to the exposure port. The amount of drug on filter membrane was quantified using UPLC-MS/MS. The following equation determined the actual dose for rats:

$$Dose(mg) = Concentration(mg/L) \times Minute\ ventilation\ of\ rat(L/min) \times Inhalation\ time(min)$$

Serial blood samples from each rat were collected from the orbital sinus at predetermined time intervals until 10 h post-dose. After centrifugation, plasma samples were harvested and stored at −70 °C. Because of the photolabile nature of RES, all these procedures were carried out under dim light conditions.

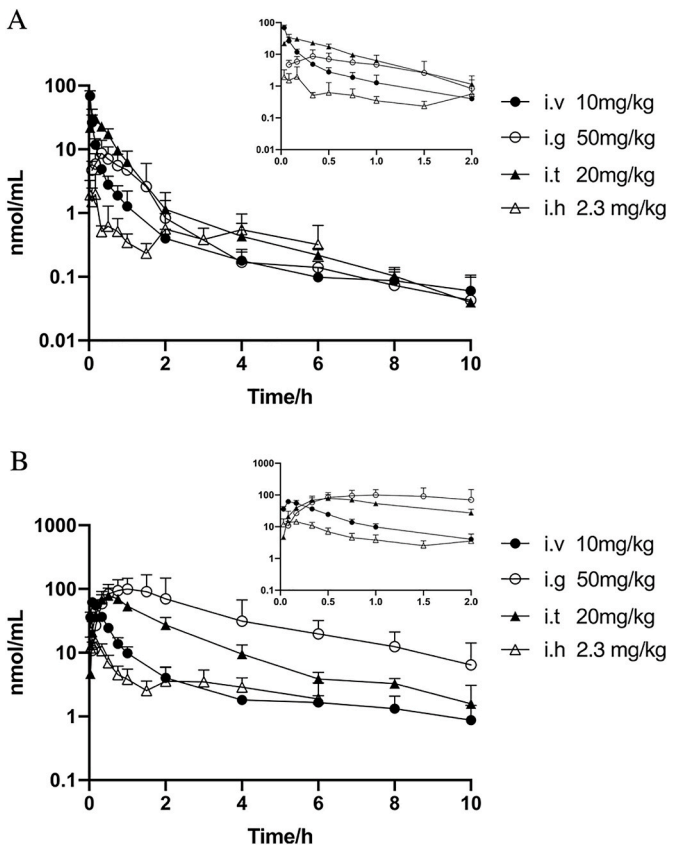

Fig. 2. Plasma mean concentration-time curves of RES (A) and R3G (B) in rats after administration of RES via i. v (10 mg/kg), i. g (50 mg/kg), i. t (20 mg/kg), and i. h (2.3 mg/kg). Inset, concentration of 0–2 h post-dose for each profile is shown. Symbols represent the mean observed values (n = 5) and the error bars represent the SD.

2.4. Biodistribution study

The biodistribution study was carried out in two groups (n = 5) to explore the differences between pulmonary (Group V) and oral administration (Group VI). The dosing route and time points for collection were determined according to results of pharmacokinetic study. Briefly, RES was delivered to rats through i. t (20 mg/kg, Group V) or i. g (50 mg/kg, Group VI) route as described above. At designed time points, animals were executed by exsanguination. Tissues were excised and collected after perfusion using saline solution. Samples were weighed quickly and homogenized using a 3-fold volume of saline to get tissue homogenate, which was stored at −70 °C until analysis.

2.5. Sample processing

The analytes were extracted using a salting-out assisted liquid-liquid extraction method according to the previous report [9]. Briefly, a 50 μL aliquot of each sample, plasma or tissue homogenate, was mixed with 100 μL methanol-acetonitrile (v/v, 3:1) working solution containing 125 ng/mL chlorzoxazone (internal standard, IS), 10 μL ascorbic acid solution (V_C, 10%), and 50 μL ammonium acetate buffer (10 M). Then, samples were vortexed adequately and centrifuged at 21,500×*g* for 10 min. After that, 50 μL aliquot of each supernatant was withdrawn and injected into the UPLC-MS/MS system for analysis. All these procedures were conducted under dim light conditions.

2.6. Metabolic study

2.6.1. Metabolic stability study

Metabolic stability study on glucuronidation of RES was carried out with rat liver microsomes (RLiM) and rat lung microsomes (RLuM). Prior to experiment, microsomes were prepared followed the previous method [14]. Incubation mixtures consisted of RLiM (0.1 mg/mL) or RLuM (0.5 mg/mL), the substrate RES (50 μM), $MgCl_2$ (10 mM), alamethicin (50 μg/mg protein) and saccharolactone (5 mM). Following preincubation for 5 min, the UDPGA (1 mM) was added to initiate metabolic reaction and mixtures (200 μL) were further incubated at 37 °C. At designed time points, an equal volume of ice-cold IS working solution (chlorzoxazone, 125 ng/mL) was added to quench the reaction. After vortex and centrifugation (21,500×*g*, 10 min), each supernatant was withdrawn and injected into UPLC-MS/MS system for analysis.

2.6.2. Enzyme kinetic study

Enzyme kinetics experiments were also carried out with RLiM and RLuM. Serial concentrations of RES in incubations ranged from 5 to 2000 μM (RLiM) or 0.2–200 μM (RLuM). Incubation mixtures were prepared as same as described above and initiated by the addition of UDPGA (1 mM), while negative control samples were also performed without either UDPGA or substrate under the same conditions. After 45 min of incubation, reaction was quenched. Samples were vortexed and centrifuged to obtain the supernatant for next analysis. All these experiments were performed under dim light condition.

2.7. UPLC-MS/MS conditions

A UPLC-MS/MS method was developed and employed to analyze RES and its metabolite (R3G) in samples. The chromatographic separation of analytes was achieved on a C18 column (150 × 2.0 mm, 2.1 μm, Shimadzu, VP-ODS) using an ultra-high-performance liquid chromatography system (LC-30 A, Shimadzu). The mobile phase consists of water (10 mM ammonium acetate, 0.05% acetic acid, phase A) and acetonitrile (phase B). The trap was eluted using a gradient of 5%–65% phase B over 5 min with a flow rate of 0.45 mL/min.

The mass spectrometry was performed in negative ionization mode using a triple quadruple tandem mass spectrometer (API 4000, AB Sciex) with MRM mode. The monitored transitions for each analyte were as follows: 227.0 → 185.0 (RES), 403.3 → 227.0 (R3G), 168.0 → 132.1 (chlorzoxazone, IS). The ion spray voltage was set at −4000 V and temperature was set at 350 °C. The nitrogen was used as the nebulizing gas, with sheath gas and auxiliary gas at 40 and 35 Arb respectively. Analyst software (version 1.6.3, AB Sciex, USA) was used for data processing and system control.

2.8. Data analysis

2.8.1. Pharmacokinetic analysis

Pharmacokinetic analysis was carried out using WinNonlin (Version 7.1, Pharsight) based on data from individual rats. The maximal plasma concentration (C_{max}) and the time to reach the peak concentration (T_{max}) were obtained directly from the measured data. Other parameters were calculated using a noncompartmental model, including the area under the concentration vs time curve (AUC), the half-life time ($T_{1/2}$), and the mean residence time (MRT). The bioavailability (F) of RES after oral or pulmonary administration was calculated as following equation:

$$F = \frac{AUC_n}{AUC_{i.v}} \times \frac{Dose_{i.v}}{Dose_n}$$

where $AUC_{i.v}$ and AUC_n represent the AUC of RES after i. v administration and other dosing routes (i.g, i. t, i. h), and $Dose_{i.\ v}$ and $Dose_n$ represent the dosage of each route.

Table 1
Plasma pharmacokinetic parameters of RES after administration of RES.

Parameters	Group I	Group II	Group III	Group IV
Dose (RES, mg/kg)	10	50	20	2.3
C_{max} (μM)	68.95 ± 14.00	8.76 ± 5.12	31.39 ± 7.18	0.65 ± 0.38
T_{max} (h)	0.033 ± 0.00	0.37 ± 0.08	0.13 ± 0.04	2.38 ± 0.75
$T_{1/2}$ (h)	2.41 ± 1.42	2.14 ± 0.94	2.78 ± 1.24	2.34 ± 1.18
$AUC_{0\text{-}t}$ (μM*h)	12.44 ± 0.98	10.32 ± 7.62	23.16 ± 2.45	1.71 ± 0.46
$AUC_{0\text{-}\infty}$ (μM*h)	12.68 ± 1.13	10.57 ± 7.71	23.57 ± 2.46	2.23 ± 0.31
MRT (h)	0.64 ± 1.34	1.27 ± 0.20	0.88 ± 0.12	1.20 ± 0.22
F (%)	–	16.68 ± 12.16	92.95 ± 9.69	76.31 ± 10.74

The route of administration for Group I-IV was i.v, i.g, i.t, and, i.h, respectively.

2.8.2. Metabolic stability analysis

As RES exhibited first-order degradation kinetics when incubated with microsomes, the *in vitro* intrinsic clearance (CL_{int}) was calculated by "*in vitro* $T_{1/2}$ method" on the basis of substrate decrease:

$$T_{1/2} = \frac{-0.693}{k}$$

where k is the graphically determined elimination rate constant of the ln (C/C_0)-t curve.

$$CL_{int} = \frac{0.693}{T_{1/2}} \times \frac{V_{incubation}}{P_{incubation}}$$

where $V_{incubation}$ and $P_{incubation}$ present the volume of incubation mixture and the amount of microsomal protein.

2.8.3. Enzymes kinetic analysis

Rates of glucuronidation of RES were described as amounts of R3G formed per minute per milligram protein (nmol/min/mg). Enzymes kinetic parameters were analyzed using GraphPad Prism (Version 8.2.0, GraphPad Software Inc.), including the maximum velocity estimate (V_{max}), Michaelis-Menten constant (K_m), and substrate inhibition constant (K_i).

2.9. Statistical analysis

Data in present study are expressed as the mean ± standard deviation (SD). Variables were found to be normally distributed and statistical analyses were performed by two-tailed unpaired *t*-test using GraphPad Prism (Version 8.2.0, GraphPad Software Inc.). Statistically significant differences were indicated when $p < 0.05$.

3. Results

3.1. Plasma pharmacokinetic profiles

The pharmacokinetic study was performed in rats following respective i. v, i. g, i. t, and i. h administration. The dose setting was on the basis of reported dose ranges in previous literatures [9,15]. Mean plasma concentration profiles of RES and R3G in rats were shown in Fig. 2. Upon i. v injection (Group I), a rapid distribution phase with an ultra-fast decline of RES was observed, followed by a prolonged elimination phase. For Group II (i.g), concentration of RES elevated to the peak (8.76 ± 5.12 μM) at 20 min post-dose and then gradually decreased. The pulmonary administration was achieved by two different delivery routes. After i. t instillation (Group III), the RES quickly entered the systemic circulation and the C_{max} (31.39 ± 7.18 μM) was recorded at 10 min. After reaching the peak, the plasma level of RES remained higher than i. v with a slow elimination trend. The profile of i. h route (Group IV) was different from the other three groups. Plasma concentration was keeping at a period of stability caused by continuous administration, and then dropped gradually. And its concentration was the lowest among all groups due to the too small dosage (2.3 mg/kg).

As shown in Fig. 2(B), RES was bio-transformed to R3G rapidly after administration. In Group I-III, plasma levels of R3G were increased with time and peaked at 5, 60, 30 min respectively, and it showed a much longer retention and higher accumulation in Group II after oral dosing. While for rats received i. h administration (Group IV), plasma levels of R3G in rats exhibited a similar behavior with RES.

The corresponding pharmacokinetic parameters of RES and R3G were listed in Tables 1 and 2. For RES, the T_{max} of i. g and i. t route was 0.37 h and 0.13 h, respectively, which suggests that RES was absorbed more quickly through the transpulmonary route than gastrointestinal route. The half-life values ($T_{1/2}$), quantifying the drug elimination from systemic circulation, were not of significant difference among these groups. The absolute bioavailability (F) was improved by pulmonary administration that F of Group III (92.95 ± 9.69%) and Group IV (76.31 ± 10.74%) were significantly higher than that of Group II (16.68 ± 12.16%). For the R3G, there was obvious plasma exposure (AUC) of R3G in all groups and no significant difference in AUC/Dose. The i. g route showed a significant higher T_{max} and $T_{1/2}$ values than i. v and i. t route, while the highest value was found in i. h route.

3.2. Influence of different administration routes on tissue distribution

Tissue distribution study was carried out following a single oral or pulmonary (i.t) administration in rats. As shown in Fig. 3(A and B), the alteration of delivery route led to the change of distribution of RES. After administration, the highest concentration was seen in the absorption organ, lung and gut respectively, at 10 min post-dosing. The maximum of AUC was also observed in lung (Group V) and gut (Group VI) among

Table 2
Plasma pharmacokinetic parameters of R3G after administration of RES.

Parameters	Group I	Group II	Group III	Group IV
Dose (RES, mg/kg)	10	50	20	2.3
C_{max} (μM)	62.08 ± 10.45	122.52 ± 65.76	82.67 ± 18.91	4.14 ± 1.82
T_{max} (h)	0.10 ± 0.04	1.00 ± 0.35	0.60 ± 0.14	2.25 ± 1.26
$T_{1/2}$ (h)	2.50 ± 1.02	4.85 ± 5.23	1.92 ± 0.38	5.12 ± 0.6
$AUC_{0\text{-}t}$ (μM*h)	50.30 ± 4.91	352.68 ± 248.18	159.41 ± 33.37	14.59 ± 7.17
$AUC_{0\text{-}\infty}$ (μM*h)	53.52 ± 4.81	455.02 ± 261.68	168.11 ± 32.91	32.98 ± 17.73
MRT (h)	1.82 ± 0.32	2.97 ± 0.93	2.03 ± 0.18	1.36 ± 0.05

The route of administration for Group I-IV was i.v, i.g, i.t, and, i.h, respectively.

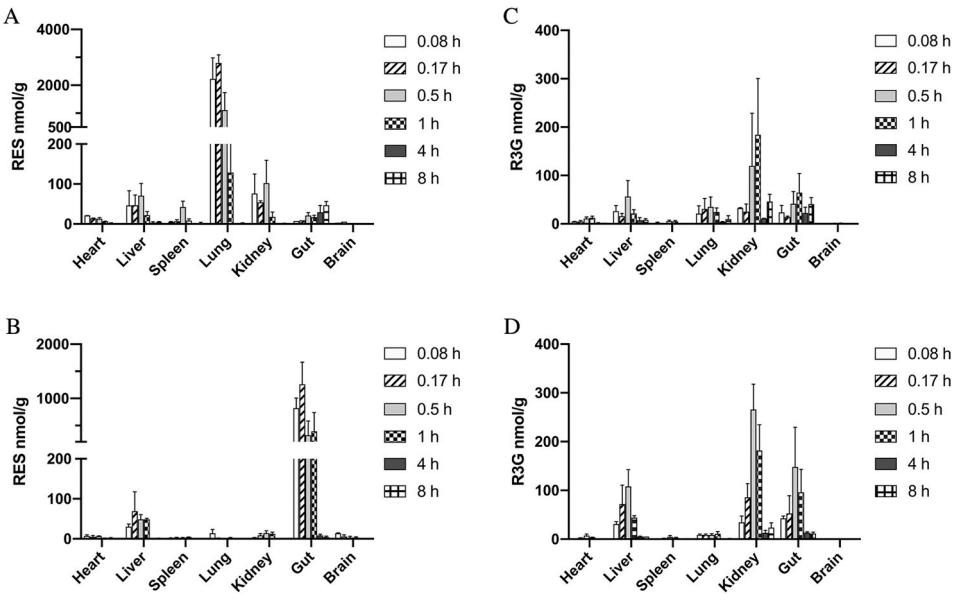

Fig. 3. Mean concentrations of RES and R3G in tissues at different time points after i. t administration of 20 mg/kg RES (A, C) and i. g administration of 50 mg/kg RES (B, D). Data were expressed as the mean ± SD, n = 5.

Table 3
$AUC_{0\text{-}t}$/Dose values of RES in different tissues of rats after i.t administration (Group V, 20 mg/kg) and i.g administration (Group VI, 50 mg/kg).

Tissue	$AUC_{0\text{-}t}$/Dose (h*nmol/g)/(mg/kg)	
	Group V	Group VI
Heart	1.62	0.33
Liver	5.21	2.67
Spleen	2.14	0.27
Lung	77.74	0.16
Kidney	5.05	0.66
Gastrointestinal tract	11.92	23.90
Brain	0.25	0.23

Table 4
Metabolic stability of RES in rat liver microsomes (RLiM) and rat lung microsomes (RLuM).

Parameters	RLiM	RLuM
k (min^{-1})	−0.017 ± 0.002	−0.003 ± 0.001
$T_{1/2}$ (min)	40.31 ± 4.79	248.81 ± 53.46
CL_{int} (μL/min/mg)	173.50 ± 19.87	5.73 ± 1.14

all these tissues. Besides, liver and kidney were another two organs sharing the largest proportion of drug exposure, accounting for almost 10% for i. t route and 12% for i. g route. The $AUC_{0\text{-}t}$/Dose values of each tissue were listed in Table 3.

The amount of R3G in different tissues were shown in Fig. 3(C and D). After i. g dosing, it was mainly distributed into the kidney, gut, and liver, reaching the maximum value at 30 min post-dosing. While for i. t administration, it was kidney that represented the highest concentration among all tested tissues, followed by the gut, lung, and liver.

3.3. Lung pharmacokinetics and deposition profiles

RES levels in lungs were shown in Fig. 4. It is evident that the lung exposure of RES was much higher after i. t dosing than that of the i. g dosing with different tendency. For i. g group, the concentration of RES was highest at 5 min post-dose and quite low at other time points. For i. t group, the concentration increased first and reached the peak level at 10 min and then gradually decreased. In the first hour after administration,

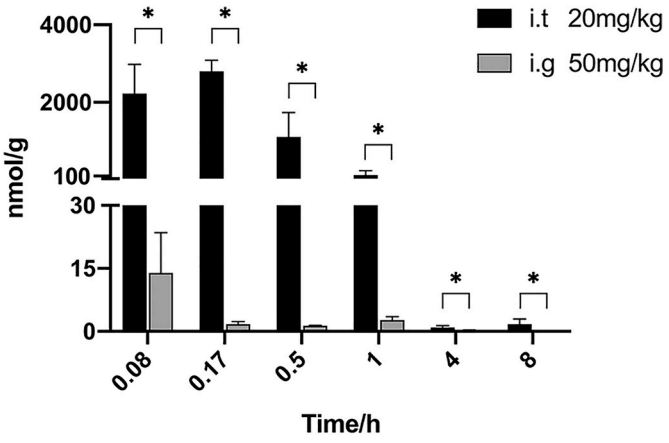

Fig. 4. Mean concentrations of RES in lungs at different time points following the administration of RES via i. t (20 mg/kg) and i. g (50 mg/kg) routes. Data were expressed as the mean ± SD, n = 5. *$p < 0.05$ indicating significantly different.

the RES concentration of i. t route was more than 100 times higher than that of i. g route. While after 4 h post-dosing, the concentration in lungs was both at a very low level for these two routes. The pharmacokinetic parameters were calculated using corresponding lung concentrations of RES in a noncompartmental manner. The $T_{1/2}$ for i. t and i. g route was 0.85 and 1.74 h, respectively.

3.4. Metabolic stability of RES in rat liver and lung microsomes

Glucuronidation of RES were probed in rat liver and lung microsomes. As shown in Fig. 5, obvious reductions were observed in incubation systems containing RLiM. These data indicated that the poor metabolic stability of RES was mainly ascribed to phase II metabolism in liver, which is consistent with previous studies [16,17]. The corresponding parameters were summarized in Table 4. Compared with RLiM, RES declined more slowly in RLuM with a longer half-life of 248.81 ± 53.46 min and a more limited CL_{int} of 5.73 ± 1.14 μL/min/mg. And the $T_{1/2}$ and CL_{int} of RLiM were 40.31 ± 4.79 min and 173.50 ± 19.87 μL/min/mg, respectively.

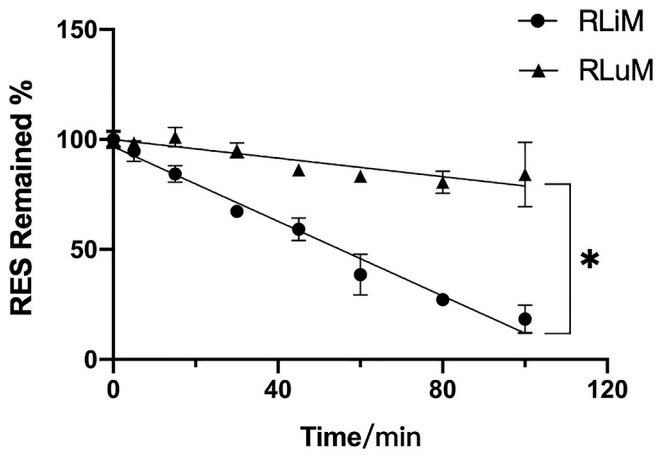

Fig. 5. Glucuronidation metabolic stability of RES in rat liver microsomes (RLiM) and rat lung microsomes (RLuM). Values represents the proportion of the residual RES in incubation mixture at different time points. Data represent the mean ± SD of triplicate determinations. *$p < 0.05$ indicating significantly different.

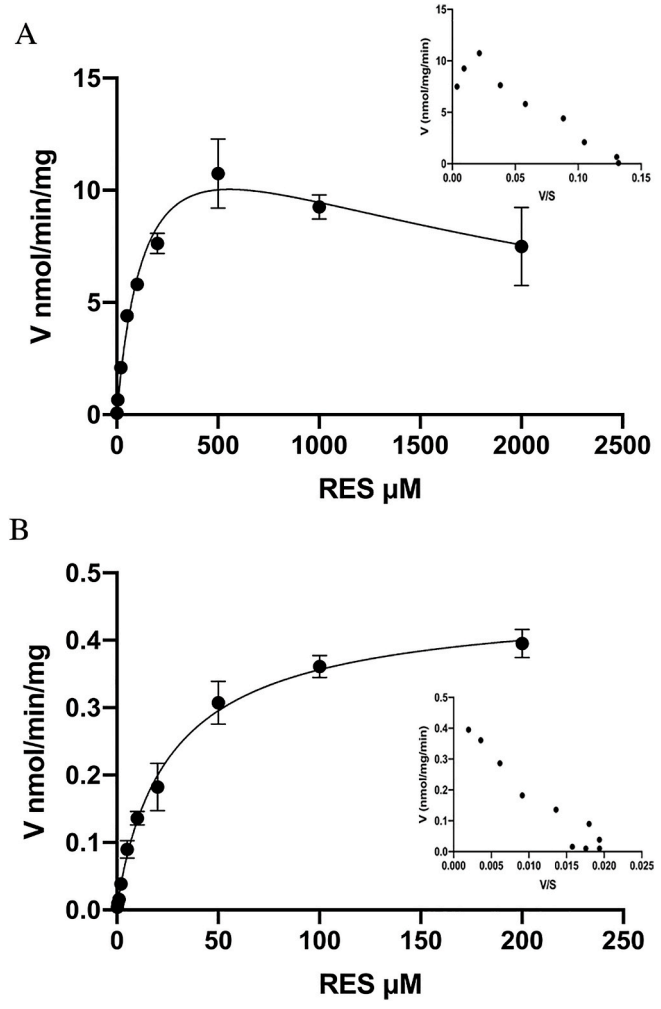

Fig. 6. Formation kinetics of R3G in rat liver microsomes (A) and rat lung microsomes (B). Inset, Eadie-Hofstee plots for each of the profiles are shown. Substrate inhibition model was selected to describe the kinetics of R3G in incubations containing RLiM. Hill model was selected for formation of R3G in incubations containing RLuM. Data were expressed as mean ± SD of triplicate determinations.

3.5. Kinetics of RES in rat liver and lung microsomes

Comparison on enzyme kinetic profiles for the formation of the R3G between RLiM and RLuM was also studied. The corresponding kinetic model for incubations was selected on the basis of visual assessment of Eadie-Hofstee plots. The coefficient of determination (R^2) was also taken into account to evaluate the fitness of each model. As depicted in Fig. 6, the liver-mediated and lung-mediated formation of R3G exhibited substrate inhibition and Hill kinetic profiles, respectively. The corresponding enzyme kinetic parameters were summarized in Table 5. Pronounced differences were observed between RLiM and RLuM. The K_m estimates for RLiM and RLuM were 156.87 ± 39.38 and 28.26 ± 6.24, respectively. Compared with hepatic metabolism (V_{max}/K_m, 102.63 ± 10.55 μL/min*mg), the lung presented negligible metabolic activity of RES (V_{max}/K_m, 17.02 ± 3.63 μL/min*mg).

4. Discussion

In this study, we explored the effectiveness of pulmonary administration on addressing limitations of RES from the perspective of pharmacokinetics. RES is a hydrophobic compound with a log $P_{O/W}$ value of 3.1 [18]. Its hydrophobicity makes it difficult to prepare an ideal aqueous solution suitable for intravenous or pulmonary administration. To increase the apparent aqueous solubility of RES and solve the problem of dissolution, RES/HP-β-CD inclusion complex was prepared and used as dosing formulation in animal experiments. HP-β-CD is a kind of cyclodextrin derivative with relatively high water solubility, minimal toxicity, and satisfactory inclusion ability [19]. It can improve the solubility of drug by forming water-soluble inclusion complexes between drug and cyclodextrin, and also increase the stability of drugs upon storage [13,20]. Previous study also demonstrated that HP-β-CD can enhance the fine particle fraction of aerosols and the drug permeation through the Calu-3 cell monolayer [20,21], which is promising for the inhaled treatment.

In order to investigate the profiles of pulmonary route, both i. t and i. h dosing route was employed. Of note, this is the first report of the use of nose-only aerosol exposure system in the pharmacokinetic study of RES. The use of this professional inhalation device is actually an effective supplement to the i. t route in the current pharmacokinetic study. Through the i. t route, rats are administered passively under anesthesia. While animals dosed via i. h route could receive the administration at a conscious condition, which is more similar to the inhaled treatments in clinic. Therefore, the i. h route is more friendly for animals and causes less damage and is more suitable for long-term administration. However, the biggest problem with this dosing route is the quite disappointing delivery efficiency of the inhalation device. In this study, even a 100 min inhalation duration was still not sufficient to provide an expected dosage. And the considerable wastage of drugs in the exposure system is also a nonnegligible defect as it requires a large amount of drug. Besides, as animals were actively inhaling the aerosolized drug in the exposure system during administration, it is difficult to precisely administer the drug to each animal. While rats in i. t group can receive precise doses according to the weight of them. Overall, the nose-only exposure system is more suitable for the further pharmacological and toxicological study, while the i. t administration was used in the following biodistribution study.

The work on pharmacokinetics was carried out first aiming to evaluate the potential role of the pulmonary administration in the bioavailability of RES. After pulmonary administration, the systemic exposure of RES was greatly increased compared to oral dosing. The absolute bioavailability was as follows: i. t (92.95 ± 9.69%) > i. h (76.31 ± 10.74%) > i. g (16.68 ± 12.16%). The remarkable enhancement of systemic exposure and bioavailability allowed for the reduction of drug dose required for its therapeutic action. Upon pulmonary and oral administrations, the T_{max} of i. t route was shorter than that of i. g route. The lag of T_{max} after i. g administration may be attributed to the

Table 5
Enzyme kinetic parameters of formation of R3G in rat liver microsomes (RLiM) and rat lung microsomes (RLuM).

Protein Source	V_{max} (nmol/mg*min)	K_m (nmol/mL)	K_i (nmol/mg*min)	V_{max}/K_m (μL/min*mg)	Model	Goodness of Fit (R^2)
RLiM	15.82 ± 2.18	156.87 ± 39.38	2119.67 ± 837.80	102.63 ± 10.55	Substrate Inhibition	0.9531
RLuM	0.47 ± 0.02	28.26 ± 6.24	–	17.02 ± 3.63	Hill (n = 0.92)	0.9880

gastric emptying. While on the other hand, the shorter absorption duration occurring in the i. t route also demonstrated that transpulmonary delivery provide a higher rate of systemic absorption compared to gastrointestinal route, which is benefited from the favorable properties of lung tissues including large surface area, extremely thin epithelium, and abundant blood flow.

The differences in biodistribution profiles of RES between pulmonary and oral administration were also explored in rats. Our experiments showed that RES was predominantly accumulated at absorption sites first after administrations and then entered the systemic circulation and distributed to other tissues. For rats received drug via i. g route, the large proportion of RES exposure detected in liver may be due to the fact that the absorbed drug can enter the liver through two pathways, both the hepatic portal vein from the intestinal tract and the hepatic artery from the systemic circulation. Previous investigations also showed that the liver is a major accumulation site for RES and its metabolites [16,22]. The evident kidney accumulations of both free RES and its metabolites were also observed, which is in line with the previous reports that renal excretion is the major route of elimination of RES [16]. As present data demonstrated, the alternation of delivery route has little impact on the excretory pattern of RES, while the further investigations is still needed.

To evaluate the effect of pulmonary administration on therapeutic action of RES for lung-specific diseases, we focused on the comparison of lung deposition of RES following pulmonary or oral administration. Because of the delivery inefficiency of the nose-only exposure system, the pulmonary administration was conducted via the i. t route. At first glance, the lung concentrations of RES appeared much higher in rats received i. t administration at each time points. The localized delivery through pulmonary route largely augment drug exposure in lungs and as a consequence improves pharmacological actions of RES in lung diseases. Additionally, the rapid accumulation in lung tissues in first 1 h is conducive for drug to exert therapeutic effects in the treatment of acute lung diseases. The decline of the concentrations in lung homogenate at 30 min post-dosing might be due to the rapid absorption and distribution equilibrium. And the quick elimination of drugs from lung tissues is conducive to reduce the toxicity for respiratory system. Noteworthily, it also appeared the tendency of distributing to lungs at 5 min after oral dosing, which might be decided by the lipophilicity of drug and the high blood flow of lungs. Lung pharmacokinetic analysis was also investigated using concentration data from lung homogenates for total lung exposures in accordance with the literature [23]. Although the i. t route achieved a higher lung accumulation in a short time, it showed a shorter $T_{1/2}$ value than i. g route. Previous investigations also showed the similar phenomena that small drugs delivered through pulmonary route have short retention times in the lungs due to the massive and rapid passage into the systemic circulation [24,25]. The aforementioned limitation thus calls for the development of effective drug delivery systems to provide a prolonged and sustained drug retention.

Extensive metabolism is a main cause of poor oral bioavailability and rapid clearance from the circulation in humans and animals [26]. Although the bioavailability has been improved greatly through pulmonary route in rats, there was still obvious plasma exposure of metabolites after pulmonary administration. Therefore, we investigated the metabolic profiles of RES *in vitro* using rat liver microsomes and lung microsomes. Overall, RES was more likely to be metabolized through phase II metabolism (glucuronidation) rather than phase I metabolism, consistent with previous reports [16,17]. And RLiM showed a much higher metabolizing activity than RLuM. These results proved our assumption that pulmonary route could be used to avoid the extensive first-pass metabolism of RES. Liver is the main accumulation site and metabolic place for RES, where the majority of the parent drug was conjugated to yield R3G, the primary metabolite in liver [8,17]. Regardless the way of administration, the absorbed RES would be distributed to liver quickly and metabolized into conjugations. And the difference of absorption rate might explain the different T_{max} of R3G in rats. The significant difference in metabolizing activity between organs could be explained by the different contributions from UGT isoforms and the expression levels of these enzymes. In humans, UGT1A1 and UGT 1A9 play a key role in catalyzing the RES glucuronidation, and UGT1A3, 1A6, 1A7, 1A8, and UGT1A10 are also capable of detectable activity on formation of metabolites [26]. Various studies have demonstrated the highly expression level of UGT1As in liver, including UGT1A1, 1A3, 1A4, 1A6, 1A9, while only UGT1A4, 1A5, 1A6 are slightly expressed in human lung tissues [27,28]. And in rats, only UGT1A6, 1A7 were detected in lungs [29]. In addition to the liver, the gastrointestinal tract is also demonstrated to be a significant metabolic organ for RES [16]. All of these results indicated that delivering the RES via pulmonary route is an effective way to avoid extensive pre-systemic metabolism and allow more drugs enter the systemic circulation.

5. Conclusion

In summary, the pharmacokinetics, tissue distribution, and metabolic profiles of RES after pulmonary administration were systematically investigated in this study. Localized delivery via pulmonary route is proved to be an effective approach for RES to improve its bioavailability by avoiding first-pass metabolism and also to deposit large accumulations at sites of action for lung diseases. These results point out the feasibility of pulmonary administration in the application of RES from the perspective of pharmacokinetics, while the pharmacodynamics of that still need further investigations. We emphasize that the application of pulmonary administration can overcome some limitations of RES as a therapeutic agent and will be a potential avenue for the clinical translation of it and other phytochemicals.

Funding

This work was supported by the Fundamental Research Funds for the Central Universities (No. 2632018PT02, No. 2632020ZD01), 'Double First-Class' initiative Innovation team project of China Pharmaceutical University (No. CPU2018GF11, No. CPU2018GY29), and Natural Science Foundation of Jiangsu Province (No. BK20190557).

Credit author statement

Dexuan Kong: Conceptualization, Formal analysis, Investigation, Writing - original draft. Chang Ren: Investigation, Visualization, Resources. Chen Ning: Investigation. Yujie Cheng: Investigation. Hui Cai: Investigation. Han Xing: Writing - review & editing. Yongjie Zhang: Writing - review & editing. Ning Li: Supervision. Yang Lu: Resources. Di Zhao: Project administration, Writing - review & editing. Xijing Chen: Conceptualization, Funding acquisition, Writing - review & editing

Declaration of competing interest

The authors report no declarations of interest.

Acknowledgement

X.C. and D.K. designed the research; D.K. and C.R. conducted the whole experiments, including sample collection and preparation, data analysis, and manuscript draft; C.N., H.C., and Y.C. participated in animal experiments; H.X. modified the manuscript; Y.Z., D.Z., and N.L. helped improve the experimental design; and X.C. and D.Z. supervised the whole experiments.

References

[1] B. Tian, J. Liu, Resveratrol: a review of plant sources, synthesis, stability, modification and food application, J. Sci. Food Agric. 100 (2020) 1392–1404, https://doi.org/10.1002/jsfa.10152.
[2] J.A. Baur, D.A. Sinclair, Therapeutic potential of resveratrol: the in vivo evidence, Nat. Rev. Drug Discov. 5 (2006) 493–506, https://doi.org/10.1038/nrd2060.
[3] A. Rauf, M. Imran, M.S. Butt, M. Nadeem, D.G. Peters, M.S. Mubarak, Resveratrol as an anti-cancer agent: a review, Crit. Rev. Food Sci. Nutr. 58 (2018) 1428–1447, https://doi.org/10.1080/10408398.2016.1263597.
[4] V. Trotta, W.-H. Lee, C.-Y. Loo, M. Haghi, P.M. Young, S. Scalia, D. Traini, In vitro biological activity of resveratrol using a novel inhalable resveratrol spray-dried formulation, Int. J. Pharm. 491 (2015) 190–197, https://doi.org/10.1016/j.ijpharm.2015.06.033.
[5] M. Elshaer, Y. Chen, X.J. Wang, X. Tang, Resveratrol: an overview of its anti-cancer mechanisms, Life Sci. 207 (2018) 340–349, https://doi.org/10.1016/j.lfs.2018.06.028.
[6] Inhalable resveratrol microparticles produced by vibrational atomization spray drying for treating pulmonary arterial hypertension, J. Drug Deliv. Sci. Technol. 29 (2015) 152–158, https://doi.org/10.1016/j.jddst.2015.07.008.
[7] T. Walle, F. Hsieh, M.H. Delegge, O.J. Jr, U.K. Walle, High absorption but very low bioavailability of oral resveratrol in humans, Drug Metab. Dispos. Biol. Fate Chem. 32 (2004) 1377, https://doi.org/10.1124/dmd.104.000885.
[8] C. Yu, Y.G. Shin, A. Chow, Y. Li, J.W. Kosmeder, Y.S. Lee, W.H. Hirschelman, J. M. Pezzuto, R.G. Mehta, R.B. van Breemen, Human, rat, and mouse metabolism of resveratrol, Pharm. Res. 19 (2002) 8.
[9] Z. Qiu, J. Yu, Y. Dai, Y. Yang, X. Lu, J. Xu, Z. Qin, F. Huang, N. Li, A simple LC-MS/MS method facilitated by salting-out assisted liquid-liquid extraction to simultaneously determine trans-resveratrol and its glucuronide and sulfate conjugates in rat plasma and its application to pharmacokinetic assay, Biomed. Chromatogr. BMC. 31 (2017), https://doi.org/10.1002/bmc.4001.
[10] H.M. Courrier, N. Butz, T.F. Vandamme, Pulmonary drug delivery systems: recent developments and prospects, Crit. Rev. Ther. Drug Carrier Syst. 19 (2002) 425, https://doi.org/10.1615/critrevtherdrugcarriersyst.v19.i45.40.
[11] J.S. Patil, S. Sarasija, Pulmonary drug delivery strategies: a concise, systematic review, Lung India off, Organ Indian Chest Soc 29 (2012) 44–49, https://doi.org/10.4103/0970-2113.92361.
[12] G. Kim, C. Piao, J. Oh, M. Lee, Self-assembled polymeric micelles for combined delivery of anti-inflammatory gene and drug to the lungs by inhalation, Nanoscale 10 (2018) 8503–8514, https://doi.org/10.1039/c8nr00427g.
[13] M.E. Davis, M.E. Brewster, Cyclodextrin-based pharmaceutics: past, present and future, Nat. Rev. Drug Discov. 3 (2014) 1023–1035.
[14] Chaorui, GuoSiqi, XueXiufen, The effect of fenofibric acid on the pharmacokinetics and pharmacodynamics of warfarin in rats, Xenobiotica (2018), https://doi.org/10.1080/00498254.2017.1306760.
[15] I.M. Kapetanovic, M. Muzzio, Z. Huang, T.N. Thompson, D.L. McCormick, Pharmacokinetics, oral bioavailability, and metabolic profile of resveratrol and its dimethylether analog, pterostilbene, in rats, Canc. Chemother. Pharmacol. 68 (2011) 593–601, https://doi.org/10.1007/s00280-010-1525-4.
[16] A. Amri, J.C. Chaumeil, S. Sfar, C. Charrueau, Administration of resveratrol: what formulation solutions to bioavailability limitations? J. Contr. Release 158 (2012) 182–193, https://doi.org/10.1016/j.jconrel.2011.09.083.
[17] P. Wang, S. Sang, Metabolism and pharmacokinetics of resveratrol and pterostilbene: resveratrol and pterostilbene, Biofactors 44 (2018), https://doi.org/10.1002/biof.1410.
[18] K. Robinson, C. Mock, D. Liang, Pre-formulation studies of resveratrol, Drug Dev. Ind. Pharm. 41 (2015) 1464–1469, https://doi.org/10.3109/03639045.2014.958753.
[19] Y. Yao, Y. Xie, C. Hong, G. Li, H. Shen, G. Ji, Development of a myricetin/hydroxypropyl-β-cyclodextrin inclusion complex: preparation, characterization, and evaluation, Carbohydr. Polym. 110 (2014) 329–337, https://doi.org/10.1016/j.carbpol.2014.04.006.
[20] V. Vartiainen, L.M. Bimbo, J. Hirvonen, E.I. Kauppinen, J. Raula, Aerosolization, drug permeation and cellular interaction of dry powder pulmonary formulations of corticosteroids with hydroxypropyl-β-cyclodextrin as a solubilizer, Pharm. Res. 34 (2017) 25–35, https://doi.org/10.1007/s11095-016-2035-9.
[21] G. Dufour, W. Bigazzi, N. Wong, F. Boschini, P. de Tullio, G. Piel, D. Cataldo, B. Evrard, Interest of cyclodextrins in spray-dried microparticles formulation for sustained pulmonary delivery of budesonide, Int. J. Pharm. 495 (2015) 869–878, https://doi.org/10.1016/j.ijpharm.2015.09.052.
[22] S. Sale, R.D. Verschoyle, D. Boocock, D.J.L. Jones, N. Wilsher, K.C. Ruparelia, G. A. Potter, P.B. Farmer, W.P. Steward, A.J. Gescher, Pharmacokinetics in mice and growth-inhibitory properties of the putative cancer chemopreventive agent resveratrol and the synthetic analogue trans 3,4,5,4′-tetramethoxystilbene, Br. J. Canc. 90 (2004) 736–744, https://doi.org/10.1038/sj.bjc.6601568.
[23] P. Paul, S. Sengupta, B. Mukherjee, T.K. Shaw, R.H. Gaonkar, M.C. Debnath, Chitosan-coated nanoparticles enhanced lung pharmacokinetic profile of voriconazole upon pulmonary delivery in mice, Nanomedicine 13 (2018) 501–520, https://doi.org/10.2217/nnm-2017-0291.
[24] J.S. Patton, P.R. Byron, Inhaling medicines: delivering drugs to the body through the lungs, Nat. Rev. Drug Discov. 6 (2007) 67–74, https://doi.org/10.1038/nrd2153.
[25] J.S. Patton, The lungs as a portal of entry for systemic drug delivery, Proc. Am. Thorac. Soc. 1 (2004) 338–344, https://doi.org/10.1513/pats.200409-049TA.
[26] M. Böhmdorfer, A. Szakmary, R. Schiestl, J. Vaquero, J. Riha, S. Brenner, T. Thalhammer, T. Szekeres, W. Jäger, Involvement of UDP-glucuronosyltransferases and sulfotransferases in the excretion and tissue distribution of resveratrol in mice, Nutrients 9 (2017) 1347, https://doi.org/10.3390/nu9121347.
[27] W. Zhang, W. Liu, F. Innocenti, M.J. Ratain, Searching for tissue-specific expression pattern-linked nucleotides of UGT1A isoforms, PloS One 2 (2007) e396, https://doi.org/10.1371/journal.pone.0000396.
[28] A. Nakamura, M. Nakajima, H. Yamanaka, R. Fujiwara, T. Yokoi, Expression of UGT1A and UGT2B mRNA in human normal tissues and various cell lines, Drug Metab. Dispos. 36 (2008) 1461–1464, https://doi.org/10.1124/dmd.108.021428.
[29] D.B. Buckley, C.D. Klaassen, Tissue- and gender-specific mRNA expression of UDP-glucuronosyltransferases (UGTs) in mice, Drug Metab. Dispos. 35 (2006) 121–127, https://doi.org/10.1124/dmd.106.012070.